Supporting information for: Mesoscale electrostatics driving particle dynamics in non-homogeneous dielectrics

Sigbjørn Løland Bore,[†] Hima Bindu Kolli,[†,§] Toshihiro Kawakatsu,[‡] Giuseppe Milano,[¶] and Michele Cascella[*,†]

†*Department of Chemistry, and Hylleraas Centre for Quantum Molecular Sciences, University of Oslo, PO Box 1033 Blindern, 0315 Oslo, Norway*

‡*Department of Physics, Tohoku University, Aoba, Aramaki, Aoba-ku, Sendai 980-8578, Japan*

¶*Department of Organic Materials Science, Yamagata University, 4-3-16 Jonan Yonezawa, Yamagata-ken 992-8510, Japan*

§*Present address: Department of Physics and Astronomy, The University of Sheffield, United Kingdom*

E-mail: michele.cascella@kjemi.uio.no

Contents

1 Derivation of external electrostatic potential

The total electrostatic energy of a system can be written as:

$$W_{\text{elec}}[\{\phi(\mathbf{r})\}, \mathbf{D}(\mathbf{r})] = \frac{1}{2}\int \mathrm{d}\mathbf{r} \frac{\mathbf{D}(\mathbf{r}) \cdot \mathbf{D}(\mathbf{r})}{\epsilon(\{\phi(\mathbf{r})\})}, \tag{1}$$

where $\mathbf{D}$ is the electrostatic displacement field. In hPF, pairwise interactions are replaced by an interaction with an external field $V_{\text{ext},k}(\mathbf{r})$, specific for the particle type. This potential is obtained through:

$$V_{\text{ext},k}(\mathbf{r}) = \frac{\delta W}{\delta \phi_k(\mathbf{r})}. \tag{2}$$

To take the functional derivative we must take into account dependence on density through $\epsilon(\mathbf{r}) = \epsilon(\{\phi(\mathbf{r})\})$ and $\mathbf{D}(\mathbf{r})$. This is done by applying the chain rule:

$$V_{\text{ext},k}(\mathbf{r}) = \int \mathrm{d}\mathbf{r}' \left(\frac{\delta W_{\text{elec}}}{\delta \mathbf{D}(\mathbf{r}')} \frac{\delta \mathbf{D}(\mathbf{r}')}{\delta \phi_k(\mathbf{r})} + \frac{\delta W_{\text{elec}}}{\delta \epsilon(\mathbf{r}')} \frac{\delta \epsilon(\mathbf{r}')}{\delta \phi_k(\mathbf{r})} \right) \tag{3}$$

or

$$V_{\mathrm{ext},k}(\mathbf{r}) = A(\mathbf{r}) + B(\mathbf{r}), \tag{4}$$

where

$$A(\mathbf{r}) \equiv \int \mathrm{d}\mathbf{r}' \frac{\delta W_{\mathrm{elec}}}{\delta \mathbf{D}(\mathbf{r}')} \frac{\delta \mathbf{D}(\mathbf{r}')}{\delta \phi_k(\mathbf{r})}, \tag{5a}$$

$$B(\mathbf{r}) \equiv \int \mathrm{d}\mathbf{r}' \frac{\delta W_{\mathrm{elec}}}{\delta \epsilon(\mathbf{r}')} \frac{\delta \epsilon(\mathbf{r}')}{\delta \phi_k(\mathbf{r})}. \tag{5b}$$

$A(\mathbf{r})$ is composed of two functional derivatives. The first part, the functional derivative of the interaction energy with respect to $\mathbf{D}$, we derive as follows:

$$\begin{aligned} \frac{\delta W_{\mathrm{elec}}}{\delta \mathbf{D}(\mathbf{r}')} &= \int \mathrm{d}\mathbf{r} \frac{\delta}{\delta \mathbf{D}(\mathbf{r}')} \frac{\mathbf{D}(\mathbf{r})\mathbf{D}(\mathbf{r})}{2\epsilon(\mathbf{r})} = \int \mathrm{d}\mathbf{r} \frac{\mathbf{D}(\mathbf{r})}{\epsilon(\mathbf{r})} \frac{\delta \mathbf{D}(\mathbf{r})}{\delta \mathbf{D}(\mathbf{r}')} \\ &= \frac{\mathbf{D}(\mathbf{r}')}{\epsilon(\mathbf{r}')} = -\boldsymbol{\nabla}' \psi(\mathbf{r}'), \end{aligned} \tag{6}$$

where $\boldsymbol{\nabla}'$ is the gradient with respect to $\mathbf{r}'$. Here, we have assumed a linear dielectric, and we have used that the displacement field can be written in terms of $\psi(\mathbf{r})$ as follows:

$$\mathbf{D}(\mathbf{r}) = -\epsilon(\mathbf{r}) \boldsymbol{\nabla} \psi(\mathbf{r}). \tag{7}$$

Next, using (6) and integration by parts, we can rewrite $A(\mathbf{r})$:

$$A(\mathbf{r}) = -\int \mathrm{d}\mathbf{r}' \boldsymbol{\nabla} \psi(\mathbf{r}') \frac{\delta \mathbf{D}(\mathbf{r}')}{\delta \phi_k(\mathbf{r})} = \int \mathrm{d}\mathbf{r}' \psi(\mathbf{r}') \boldsymbol{\nabla} \cdot \frac{\delta \mathbf{D}(\mathbf{r}')}{\delta \phi_k(\mathbf{r})}. \tag{8}$$

The Maxwell equation for displacement field, with explicit density dependence of charge density $\rho(\mathbf{r})$ gives:

$$\boldsymbol{\nabla} \cdot \mathbf{D}(\mathbf{r}) = \rho(\mathbf{r}) = \sum_{k=1}^{M} \phi_k(\mathbf{r}) q_k. \tag{9}$$

From (9), assuming operations commute, we apply functional derivative and obtain:

$$\boldsymbol{\nabla} \cdot \frac{\delta \mathbf{D}(\mathbf{r})}{\delta \phi_k(\mathbf{r}')} = q_k \delta(\mathbf{r} - \mathbf{r}'). \tag{10}$$

Using (10), we get the full expression:

$$A(\mathbf{r}) = \int \mathrm{d}\mathbf{r}' \psi(\mathbf{r}') q_k \delta(\mathbf{r} - \mathbf{r}') = q_k \psi(\mathbf{r}). \tag{11}$$

Assuming local dependence of ϵ on ϕ_k, (5) can be written as:

$$B(\mathbf{r}) = \frac{\partial \epsilon(\mathbf{r})}{\partial \phi_k(\mathbf{r})} \frac{\delta W_{\mathrm{elec}}}{\delta \epsilon(\mathbf{r})}, \tag{12}$$

The functional derivative in (12) is obtained by:

$$\begin{aligned} \frac{\delta W_{\mathrm{elec}}}{\delta \epsilon(\mathbf{r})} &= \frac{\delta}{\delta \epsilon(\mathbf{r})} \frac{1}{2} \int \mathrm{d}\mathbf{r}' \frac{\mathbf{D}(\mathbf{r}') \cdot \mathbf{D}(\mathbf{r}')}{\epsilon(\mathbf{r}')} \\ &= \frac{1}{2} \int \mathrm{d}\mathbf{r}' \mathbf{D}(\mathbf{r}') \cdot \mathbf{D}(\mathbf{r}') \frac{\partial}{\partial \epsilon(\mathbf{r}')} \left(\frac{1}{\epsilon(\mathbf{r}')} \right) \frac{\delta \epsilon(\mathbf{r}')}{\delta \epsilon(\mathbf{r})} \\ &= -\frac{1}{2} \int \mathrm{d}\mathbf{r}' \frac{\mathbf{D}(\mathbf{r}') \cdot \mathbf{D}(\mathbf{r}')}{\epsilon(\mathbf{r}')^2} \delta(\mathbf{r} - \mathbf{r}') \\ &= -\frac{1}{2} \frac{\mathbf{D}(\mathbf{r}) \cdot \mathbf{D}(\mathbf{r})}{\epsilon(\mathbf{r})^2}, \end{aligned} \tag{13}$$

where we used that

$$\frac{\delta \epsilon(\mathbf{r}')}{\delta \epsilon(\mathbf{r})} = \delta(\mathbf{r} - \mathbf{r}'). \tag{14}$$

Inserting (13) into (5a), we find:

$$B(\mathbf{r}) = -\frac{1}{2} \frac{\partial \epsilon(\mathbf{r})}{\partial \phi_k(\mathbf{r})} \frac{\mathbf{D}(\mathbf{r}) \cdot \mathbf{D}(\mathbf{r})}{\epsilon(\mathbf{r})^2} \tag{15}$$

Finally, the external potential can be written as:

$$V_{\mathrm{ext},k} = q_k \psi(\mathbf{r}) - \frac{1}{2} \frac{\partial \epsilon(\mathbf{r})}{\partial \phi_k(\mathbf{r})} (\boldsymbol{\nabla} \psi(\mathbf{r}))^2. \tag{16}$$

2 Relationship to the Helmholtz force density

Focusing on polarization term, the force contribution to a volume can be written as:

$$\mathbf{F} = \frac{1}{2}\int \mathrm{d}\mathbf{r} \sum_k \phi_k(\mathbf{r}) \boldsymbol{\nabla} \left(\frac{\partial \epsilon(\mathbf{r})}{\partial \phi_k} (\boldsymbol{\nabla}\psi(\mathbf{r}))^2 \right), \tag{17}$$

Using the product rule, we obtain

$$\mathbf{F} = \frac{1}{2}\int \mathrm{d}\mathbf{r} \sum_k \left(\boldsymbol{\nabla}(\phi_k(\mathbf{r}) \frac{\partial \epsilon(\mathbf{r})}{\partial \phi_k} (\boldsymbol{\nabla}\psi(\mathbf{r}))^2) - \boldsymbol{\nabla}\phi_k(\mathbf{r}) \frac{\partial \epsilon(\mathbf{r})}{\partial \phi_k} (\boldsymbol{\nabla}\psi(\mathbf{r}))^2 \right). \tag{18}$$

Equation (18) can be rewritten, by using

$$\boldsymbol{\nabla}\epsilon(\mathbf{r}) = \sum_k \boldsymbol{\nabla}\phi_k(\mathbf{r}) \frac{\partial \epsilon(\mathbf{r})}{\partial \phi_k}, \tag{19}$$

as:

$$\mathbf{F} = \frac{1}{2}\int \mathrm{d}\mathbf{r} \left(\boldsymbol{\nabla} \left(\sum_{\mathrm{k}} \phi_{\mathrm{k}}(\mathbf{r}) \frac{\partial \epsilon(\mathbf{r})}{\partial \phi_{\mathrm{k}}} (\boldsymbol{\nabla}\psi(\mathbf{r}))^2 \right) - \boldsymbol{\nabla}\epsilon(\mathbf{r}) (\boldsymbol{\nabla}\psi(\mathbf{r}))^2 \right). \tag{20}$$

The force density per volume is given by the integrand:

$$\mathbf{f}_{\mathrm{pol}} = \frac{1}{2}\boldsymbol{\nabla} \left(\sum_k \phi_k(\mathbf{r}) \frac{\partial \epsilon(\mathbf{r})}{\partial \phi_k} (\boldsymbol{\nabla}\psi(\mathbf{r}))^2 \right) - \frac{1}{2}\boldsymbol{\nabla}\epsilon(\mathbf{r}) (\boldsymbol{\nabla}\psi(\mathbf{r}))^2, \tag{21}$$

which for a single-component fluid is the Helmholtz force density.[S1] We note that, for a weighted average for $\epsilon(\mathbf{r})$, the first term sum to zero.

3 Numerical solution of GPE

A regular grid with periodic boundary conditions is used with box of size $L_x \times L_y \times L_z$ discretized by N_x, N_y and N_z points in each direction respectively. The position of the nodes are given by $x_i = i \cdot \Delta x$, $y_j = j \cdot \Delta y$, $z_k = k \cdot \Delta z$, where $\Delta x \equiv L_x/N_x$, $\Delta y \equiv L_y/N_y$ and $\Delta z \equiv L_z/N_z$. On the nodes, $\epsilon(\mathbf{r})$, $\rho(\mathbf{r})$, $\psi(\mathbf{r})$ are discretized as $\epsilon_{i,j,k}$, $\rho_{i,j,k}$, $\psi_{i,j,k}$. We

derive a finite difference scheme by approximating derivatives in GPE with central differences on half points between nodes:

$$\begin{aligned}
&\frac{1}{\Delta x}\left(\left(\epsilon\frac{\partial\psi}{\partial x}\right)_{i+1/2,j,k}-\left(\epsilon\frac{\partial\psi}{\partial x}\right)_{i-1/2,j,k}\right)+\\
&\frac{1}{\Delta y}\left(\left(\epsilon\frac{\partial\psi}{\partial y}\right)_{i,j+1/2,k}-\left(\epsilon\frac{\partial\psi}{\partial y}\right)_{i,j-1/2,k}\right)+\\
&\frac{1}{\Delta z}\left(\left(\epsilon\frac{\partial\psi}{\partial z}\right)_{i,j,k+1/2}-\left(\epsilon\frac{\partial\psi}{\partial z}\right)_{i,j,k-1/2}\right)=-\rho_{i,j,k},
\end{aligned} \tag{22}$$

which gives

$$\begin{aligned}
&\frac{1}{\Delta x^2}\left(\epsilon_{i+1/2,j,k}(\psi_{i+1,j,k}-\psi_{i,j,k})-\right.\\
&\qquad\left.\epsilon_{i-1/2,j,k}(\psi_{i,j,k}-\psi_{i-1,j,k})\right)+\\
&\frac{1}{\Delta y^2}\left(\epsilon_{i,j+1/2,k}(\psi_{i,j+1,k}-\psi_{i,j,k})-\right.\\
&\qquad\left.-\epsilon_{i,j-1/2,k}(\psi_{i,j,k}-\psi_{i,j-1,k})\right)+\\
&\frac{1}{\Delta z^2}\left(\epsilon_{i,j,k+1/2}(\psi_{i,j,k+1}-\psi_{i,j,k})-\right.\\
&\qquad\left.\epsilon_{i,j,k-1/2}(\psi_{i,j,k}-\psi_{i,j,k-1})\right)=-\rho_{i,j,k},
\end{aligned} \tag{23}$$

where

$$\epsilon_{i+1/2,j,k}\equiv\frac{1}{2}\left(\epsilon_{i+1,j,k}+\epsilon_{i,j,k}\right). \tag{24}$$

GPE can be rewritten in finite difference form as follows:

$$\begin{aligned}
&a_1\psi_{i+1,j,k}+a_2\psi_{i-1,j,k}+\\
&a_3\psi_{i,j+1,k}+a_4\psi_{i,j-1,k}+\\
&a_5\psi_{i,j,k+1}+a_6\psi_{i,j,k-1}-\\
&\qquad a_0\psi_{i,j,k}=-\rho_{i,j,k},
\end{aligned} \tag{25}$$

where we identify the a_k from equation (23) as:

$$a_1 = \frac{1}{2\Delta x^2}\left(\epsilon_{i-1,j,k} + \epsilon_{i,j,k}\right), \tag{26a}$$

$$a_2 = \frac{1}{2\Delta x^2}\left(\epsilon_{i,j,k} + \epsilon_{i+1,j,k}\right), \tag{26b}$$

$$a_3 = \frac{1}{2\Delta y^2}\left(\epsilon_{i,j-1,k} + \epsilon_{i,j,k}\right), \tag{26c}$$

$$a_4 = \frac{1}{2\Delta y^2}\left(\epsilon_{i,j,k} + \epsilon_{i,j+1,k}\right), \tag{26d}$$

$$a_5 = \frac{1}{2\Delta z^2}\left(\epsilon_{i,j,k-1} + \epsilon_{i,j,k}\right), \tag{26e}$$

$$a_6 = \frac{1}{2\Delta z^2}\left(\epsilon_{i,j,k} + \epsilon_{i,j,k+1}\right), \tag{26f}$$

and

$$a_0 = a_1 + a_2 + a_3 + a_4 + a_4 + a_6. \tag{27}$$

Solving equation (25) is equivalent to solving a system of banded linear equations, for which many methods exist (note that the accuracy is not related to the method for solving the set of equations, but the finite difference discretization). Widely used methods include Multigrid method,[S2] Conjugate gradient,[S3] or relaxation methods like Jacobi, Gauss-Seidel and successive over relaxation (SOR).[S3] Here, we employ SOR because of good efficiency and ease of implementation.

The SOR-method solves GPE iteratively by:

$$\psi^{n+1}_{i,j,k} = (1-\omega)\psi^{n}_{i,j,k} + \frac{\omega}{a_0}\left(\rho_{i,j,k} + a_1\psi^{n}_{i+1,j,k} + .a_2\psi^{n}_{i-1,j,k} + a_3\psi^{n}_{i,j+1,k} + a_4\psi^{n}_{i,j-1,k} + a_5\psi^{n}_{i,j,k+1} + a_6\psi^{n}_{i,j,k-1}\right), \tag{28}$$

where n is marks the number of iterations and ω is a relaxation parameter crucial for the convergence-rate. We use $\omega = 2.0/(1.0 + \sin(\pi/N_x))$ in accordance with.[S4] As convergence criteria we employ:

$$\left\langle \left|\psi^{n+1}_{i,j,k} - \psi^{n}_{i,j,k}\right| \right\rangle < 1 \times 10^{-6}\,\mathrm{mV}. \tag{29}$$

The number of iterations required for for convergence is dependent on system and the time δt between potential updates. Figure S1 provides the number of iterations N_{it} required for achieving (29) for a charge lipid bilayer.

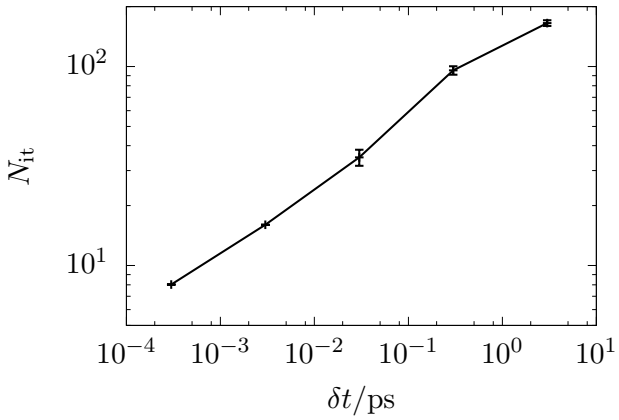

Figure S1: Mean number of steps required for convergence as function of time δt between potential updates. This particular convergence test was performed on a equilibrated charged lipid bilayer with $\epsilon_{1,80}$. Details on this system are reported in Appendix 4.2.

4 Simulation details

Settings used for molecular dynamics are provided in Table S1. All simulations are done under periodic boundary conditions

Table S1: Settings used in OCCAM simulations.

Δt^a/ps	δt^b/ps	δt^c/ps	$f_{\mathrm{col}}{}^d$/ps^{-1}	T/K	b/nm	κ^{-1}/kJ mol^{-1}
0.03	3	0.3	7	301.15	0.65	20

[a] Time step.
[b] Time between grid update for partitioning simulations.
[c] Time between grid update for membrane simulations.
[d] Collision frequency of Andersen thermostat.

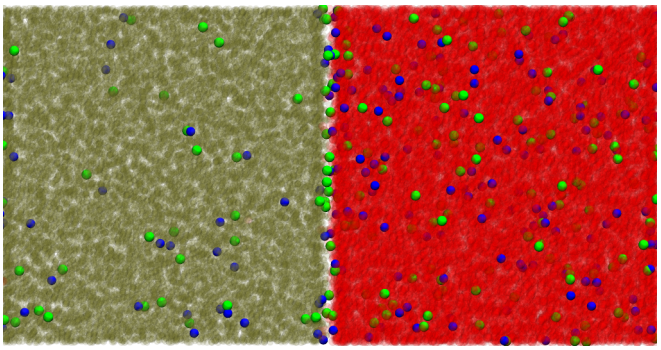

Figure S2: Random snapshot from a hPF-MD/e simulation of a 200 mM salt concentration in a oil/water bi-phase solution, using $\epsilon_o = 10$. The oil beads are colored in dark green, the water beads in red; positive and negative ions are represented by light green and blue spheres.

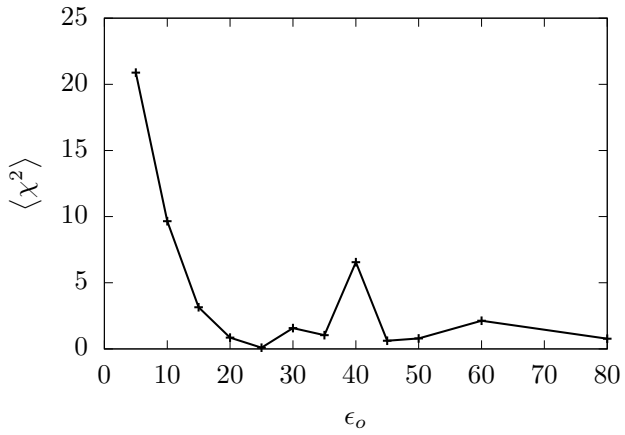

Figure S3: The $\langle \chi^2 \rangle$ of fitting for concentration dependence of $D_{o/W}$ for different ϵ_o.

4.1 Partitioning simulations

The partitioning simulations are done in a box of dimensions 29.8 nm × 14.9 nm × 14.9 nm, starting phase separated with oil on left side ($x < 14.9$ nm) and water on right side (14.9 nm $< x <$ 29.8 nm). The initial phase separation is maintained throughout the simulation by $\chi_{o,w} \times RT = 30\,\mathrm{kJ\,mol^{-1}}$. Ions are only subject to compressibility condition and electrostatic interactions $\chi_{\mathrm{ion,j}} \times RT = 0$. The simulations are performed with $\epsilon_w = 80$, $\epsilon_{\mathrm{ion}} = 80$ and $\epsilon_o = \{5, 10, 15, 20, 25, 35, 40, 45, 50, 60, 80\}$. All beads are set to a mass 72 amu. The simulations last for a total time $t = 0.97\,\mu$s. The distribution coefficient is calculated by the

time average:

$$D_{o/w} = \frac{1}{n_{\text{frames}}} \sum_{i=1}^{n_{\text{frames}}} \frac{N^i_{A^+o} + N^i_{B^-o}}{N^i_{A^+w} + N^i_{B^-w}}, \tag{30}$$

where the number of ions in each phase are counted away from the interface. The corresponding standard deviations of the mean are estimated using block averaging.[S5] For each ϵ_o from concentration dependence of $D_{o/w}$, equilibria constants are obtained by optimizing:

$$\langle \chi^2 \rangle = \left\langle \left(\frac{(\log D_{o/w} - \log D_{o/w,\text{fit}}}{\sigma_{\log D_{o/w},}} \right)^2 \right\rangle \tag{31}$$

for equilibria constants, constraining $K_w = 250\,\text{mM}$. The $\langle \chi^2 \rangle$ for different ϵ_o are reported in Figure S3.

Table S2: System setup for ion concentration dependence of partitioning. The simulation box is $29.8 \times 14.9 \times 14.9$ nm^3 and there are 55200 solvent beads (27600 oil and 27600 water beads). $N_{\text{A}^+\text{B}^-}$ denotes number of A^+ and B^- ions.

c_{ion}/mM	5	10	25	50	100	150	200
$N_{\text{A}^+\text{B}^-}$	20	40	100	200	400	600	800

4.2 Membrane simulations

Table S3: $\chi_{ij} \times RT/\text{kJ mol}^{-1}$-matrix for membrane simulations.

	L	P	G	C	D	A^+	B^-	W
L	0.00	-3.60	4.50	13.25	9.30	0.00	0.00	0.00
P	-3.60	0.00	4.50	13.50	11.70	0.00	0.00	-3.60
G	4.50	4.50	0.00	6.30	6.30	0.00	0.00	4.50
C	13.25	13.50	6.30	0.00	0.00	0.00	0.00	33.75
D	9.30	11.70	6.30	0.00	0.00	0.00	0.00	23.25
A^+	0.00	0.00	0.00	0.00	0.00	0.00	0.00	0.00
B^-	0.00	0.00	0.00	0.00	0.00	0.00	0.00	0.00
W	0.00	-3.60	4.50	33.75	23.25	0.00	0.00	0.00

The ion membrane simulations are performed with lipid positions frozen in time. The initial setup for the bilayer are made using *insane*,[S6] a tool for creating initial setup for

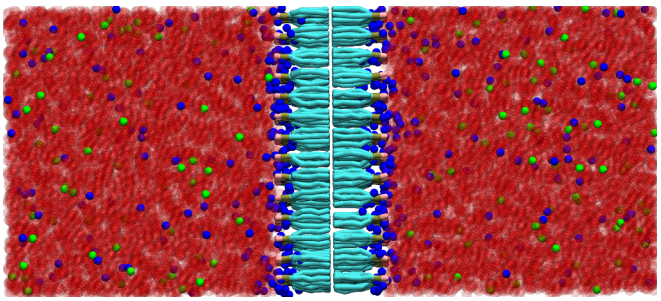

Figure S4: Snapshot of membrane simulation for charged lipid bilayer with salt. $\epsilon_{mem} = 1$ and $\epsilon_w = 80$. Water beads are colored in red, A^+ and B^- ions are represented by light green and blue spheres. The lipids are represented in sticks.

membranes. The polar/charged bilayers are composed of 391/392 lipids, respectively, placed along the xy-plane of a simulation box of $10.18 \times 10.18 \times 23.29\,\mathrm{nm}^3$ dimensions. The polar membrane was simulated in the presence of 145 A^+B^- ion couples, and 15887 water beads. The charged system contained 537 A^+ and 145 B^- ions, as well as 15495 waters. The χ_{ij}-matrix used for modeling intermolecular interactions is provided in Table S3. A snapshot of the simulation setup for a charged membrane is shown in Figure S4.

References

(S1) Brevik, I. Experiments in phenomenological electrodynamics and the electromagnetic energy-momentum tensor. *Phys. Rep.* **1979**, *52*, 133–201.

(S2) Holst, M.; Saied, F. Multigrid solution of the PoissonBoltzmann equation. *J. Comput. Chem.* **1993**, *14*, 105–113.

(S3) Davis, M. E.; McCammon, J. A. Solving the finite difference linearized Poisson-Boltzmann equation: A comparison of relaxation and conjugate gradient methods. *J. Comput. Chem.* **1989**, *10*, 386–391.

(S4) Yang, S.; Gobbert, M. K. The optimal relaxation parameter for the SOR method applied to the Poisson equation in any space dimensions. *Appl. Math. Lett.* **2009**, *22*, 325–331.

(S5) Flyvbjerg, H.; Petersen, H. G. Error estimates on averages of correlated data. *J. Chem. Phys.* **1989**, *91*, 461–466.

(S6) Wassenaar, T. A.; Ingólfsson, H. I.; Böckmann, R. A.; Tieleman, D. P.; Marrink, S. J. Computational Lipidomics with insane: A Versatile Tool for Generating Custom Membranes for Molecular Simulations. *J. Chem. Theory Comput.* **2015**, *11*, 2144–2155.